

## Supporting Information

### **Robust and Efficient UV-reflecting One-Dimensional Photonic Crystals Enabled by Organic/Inorganic Nanocomposite Thin Films for Photoprotection of Transparent Polymers**

*Junli Zhang<sup>1,2</sup>, Shengjie Xi<sup>1</sup>, Guangyu Mao<sup>1</sup>, Rui Yin<sup>1</sup>, Lin Zhu<sup>1</sup>, Dengyang Li<sup>1</sup>, Zhiqiang Yao<sup>2</sup>, Hao-Yang Mi<sup>1\*</sup>, Jian Han<sup>1\*</sup>, Chuntai Liu<sup>1</sup>, Changyu Shen<sup>1</sup>*

<sup>1</sup>National Engineering Research Center for Advanced Polymer Processing Technology, Key Laboratory of Materials Processing and Mold, Zhengzhou University, Zhengzhou, 450000, China

<sup>2</sup>School of Materials Science and Engineering, Zhengzhou University, Zhengzhou, 450000, China

## 1. Supporting Experimental Details

### 1.1 Fabrication of PC sheet

Bare PC sheets with dimension of  $100 \times 100 \times 3 \text{ mm}^3$  were injection-molded by HTF80-W2 (Haitian, China) with a processing temperature of  $280 \text{ }^\circ\text{C}$ , a mold temperature of  $80 \text{ }^\circ\text{C}$ , and an injection pressure of 100 MPa. And then, PC sheets were cut into small pieces of  $25 \times 25 \text{ mm}^2$  using a saw and annealed at  $120 \text{ }^\circ\text{C}$  for 4 h in an oven.

### 1.2 Supporting characterization details

The chemical composition of PC sheets was measured both before and after UVC treatment using Fourier transform infrared spectroscopy (FTIR, Nicolet 6700, Thermoscientific, USA). Water contact angle (WCA) was evaluated using a dynamic/static optical contact angle meter (SL200B/K, Kino, USA). Digital photographs were taken by a digital camera (Canon EOS 2000D). The surface morphology of as-prepared 1DPhC film on PC was observed by polarization microscope (OlympusBX61). The morphology of nanoparticles in  $\text{TiO}_2$  sol,  $\text{SiO}_2$  sol and their O/I hybrid sols were observed using transmission electron microscope (TEM, FEI Tecnai G2 F20). The absorbance spectra of UV-reflecting  $\text{GTS}_{50}$  1DPhC films coated PC before and after UVB aging test were recorded by a UV-vis-NIR spectrophotometer (PerkinElmer Lambda 1050).

### 1.3 Supporting theoretical analysis

Regarding thicknesses of high-index and low-index layers as fitting parameters, Monte Carlo method<sup>1</sup> in combination with the TMM model<sup>2</sup> was used to fit the experimental reflectance spectra until the correlation coefficient ( $r$ ) between the simulated and measured reflectance spectra was greater than 0.85. The  $r$  was defined by the following equation (1):

$$r = 1 - \frac{\sum_{\lambda=280}^{800} (R_{\lambda} - R_{\lambda}^0)^2}{\sum_{\lambda=280}^{800} R_{\lambda}^2} \quad (1)$$

where  $R_{\lambda}$  and  $R_{\lambda}^0$  were the experimental and theoretical reflectance at the wavelength of  $\lambda$ , respectively. The obtained theoretical layer thickness was also cross-checked with measured results from the corresponding FESEM image.

## 2. Supporting Figures

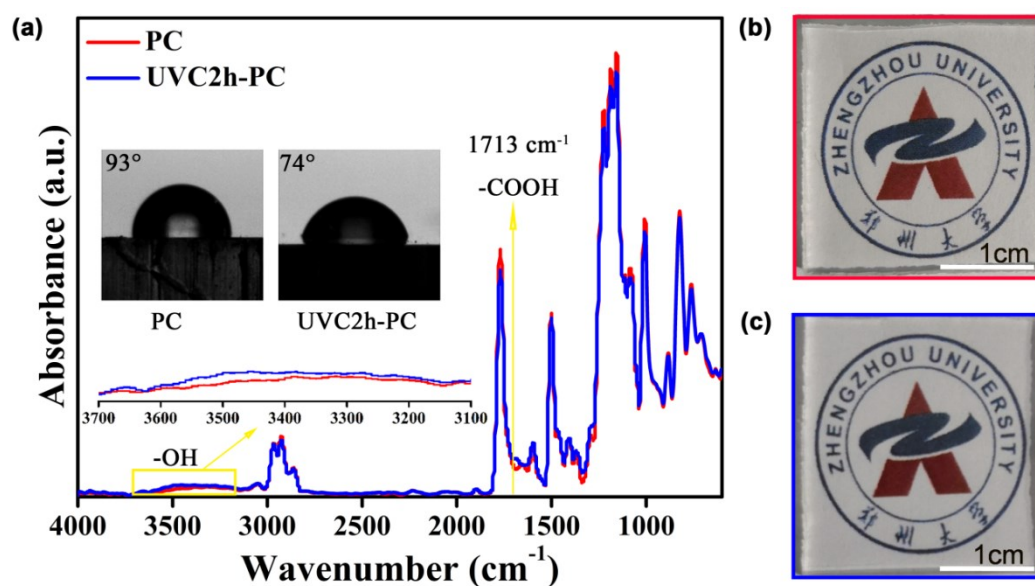


**Fig. S1** (a) FTIR spectra of PC substrate before and after UVC irradiation pretreatment for 2 h (inset images are water contact angles of their corresponding surfaces); (b) and (c) are their corresponding digital photographs.

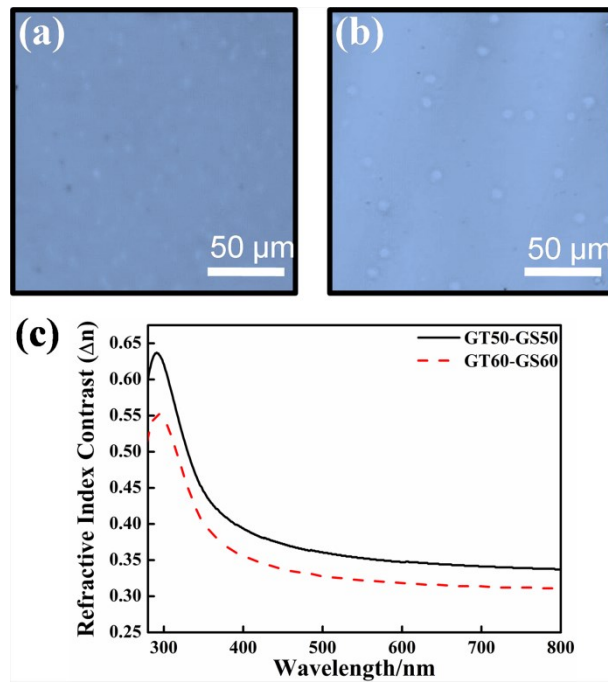


**Fig. S2** Optical microscope images of (a) GTS<sub>50</sub> and (b) GTS<sub>60</sub> 1DPhC films coated PC; (c) Refractive index contrasts ( $\Delta n$ ) between GT<sub>50</sub> and GS<sub>50</sub> and between GT<sub>60</sub> and GS<sub>60</sub>, respectively, in the wavelength range of 280-800 nm.

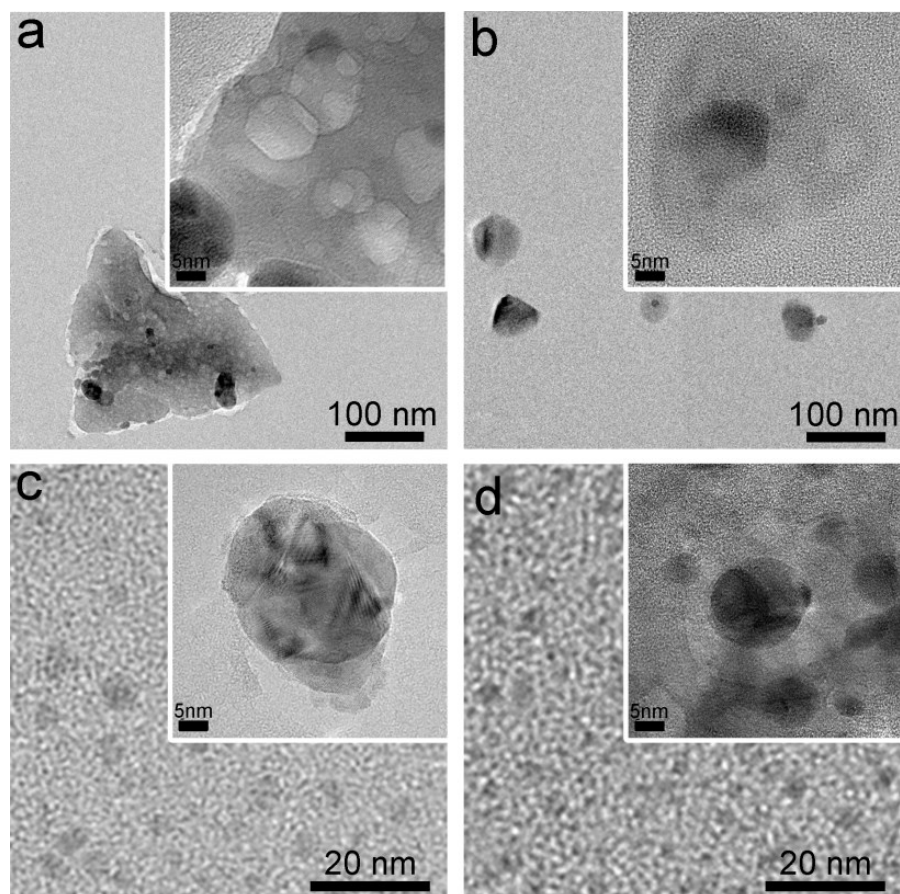


**Fig. S3** TEM images of (a) SiO<sub>2</sub> sol, (b) GS<sub>50</sub> sol, (c) TiO<sub>2</sub> sol and (d) GT<sub>50</sub> sol. The inset images are their corresponding enlarged views.

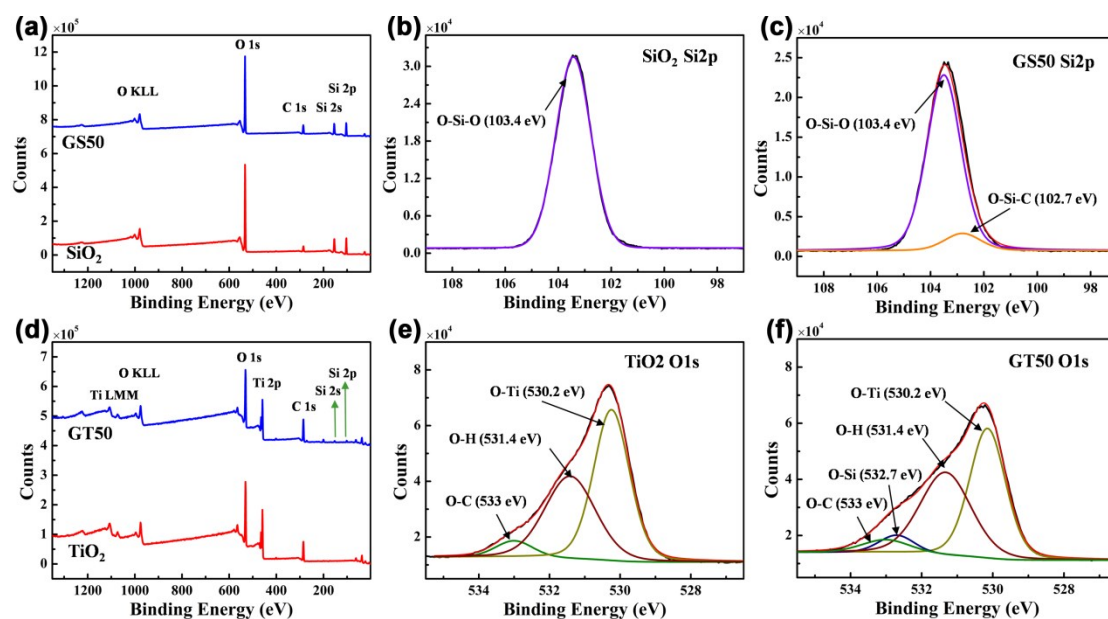


**Fig. S4** XPS spectra of  $\text{SiO}_2$  and  $\text{GS}_{50}$  (a) survey scan, and high resolution  $\text{Si}2p$  scan of (b)  $\text{SiO}_2$  and (c)  $\text{GS}_{50}$ ; XPS spectra of  $\text{TiO}_2$  and  $\text{GT}_{50}$  (d) survey scan, and high resolution  $\text{O}1s$  scan of (e)  $\text{TiO}_2$  and (f)  $\text{GT}_{50}$ .

XPS measurements were performed to gain further insight into the chemical structure of  $\text{GS}_{50}$  and  $\text{GT}_{50}$  nanocomposites by comparing them with  $\text{SiO}_2$  and  $\text{TiO}_2$ . As shown in Fig.S4a, C, Si, and O elements were detected from  $\text{GS}_{50}$  and  $\text{SiO}_2$ , and the C1s peak intensity of  $\text{GS}_{50}$  was much greater than that of  $\text{SiO}_2$  suggesting the successful modification of GPTMS. Moreover, the high resolution  $\text{Si}2p$  peak was Gauss fitted to indicate the composition of chemical bonds. It was found from Fig. S4 b and c that  $\text{SiO}_2$  contains O–Si–O (103.4 eV) bond<sup>3</sup> only, while  $\text{GS}_{50}$  is composed of O–Si–C(102.7eV) and O–Si–O (103.4 eV) bonds. These results provide evidence for the covalent linkage between  $\text{SiO}_2$  nanoparticles and GPTMS molecules<sup>4</sup>. Figure S4d shows the survey scan of  $\text{TiO}_2$  and  $\text{GT}_{50}$ . It is clear that not only the C1s peak intensity was increased with the GPTMS modification, but also two characteristic peaks belonged to Si2s and Si2p were appeared on  $\text{GT}_{50}$ . These features demonstrated that organosilane has been incorporated into  $\text{TiO}_2$  as well. High resolution  $\text{O}1s$  peaks are also fitted as shown in Fig. S4e and f.  $\text{TiO}_2$  showed three typical bonds that are

assigned to O–Ti (530.2 eV), O–C (531.4 eV) and O–H (533 eV), respectively<sup>5</sup>, suggesting successful synthesis of TiO<sub>2</sub>. However, a peak assigned to O–Si (532.7 eV) appeared on the O1s curve of GT<sub>50</sub> indicating the formation of Ti–O–Si and Si–O–Si bonds<sup>6</sup>, which confirmed that GPTMS molecules have been covalently bonded to TiO<sub>2</sub> nanoparticles and undergone self-condensation reaction.

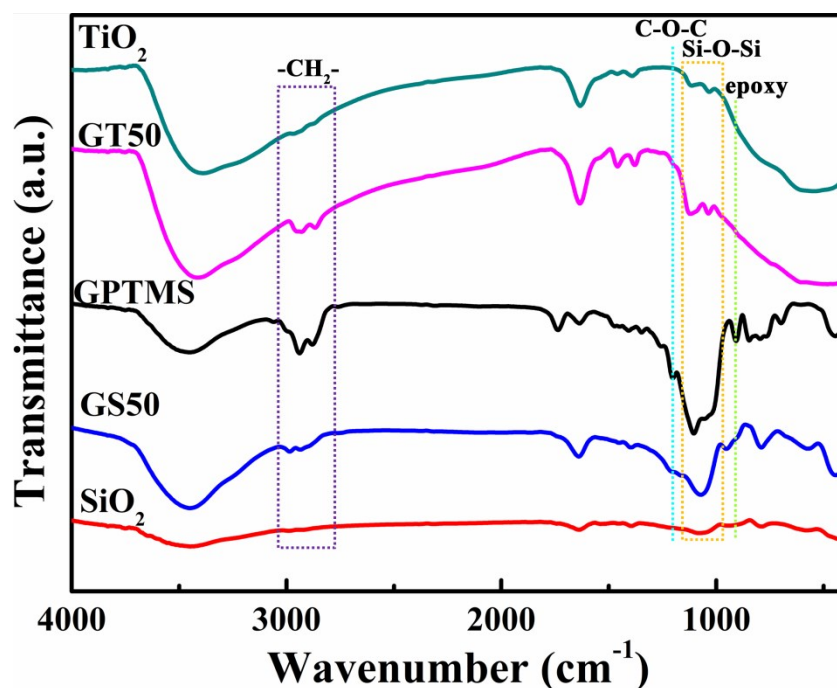


**Fig. S5** FTIR spectra of  $\text{TiO}_2$ ,  $\text{GT}_{50}$ , GPTMS,  $\text{GS}_{50}$  and  $\text{SiO}_2$

To further confirm the formation of organosilicate network, FTIR measurements of  $\text{TiO}_2$ ,  $\text{SiO}_2$ , GPTMS, and  $\text{GT}_{50}$  and  $\text{GS}_{50}$  hybrid nanocomposites were performed. As shown in Fig. S5, the absorption peaks at  $622\text{ cm}^{-1}$  in  $\text{TiO}_2$  spectrum and  $1080\text{ cm}^{-1}$  in  $\text{SiO}_2$  spectrum were corresponding to the stretching vibration of  $\text{Ti-O-Ti}$  and  $\text{Si-O-Si}$  bonds, respectively, which were generated by the condensation reaction of hydrolyzed TBT and TEOS<sup>6, 7</sup>. After being modified with GPTMS, it is obvious that both  $\text{GT}_{50}$  and  $\text{GS}_{50}$  spectra showed the characteristic peaks at  $2938\text{ cm}^{-1}$  and  $2879\text{ cm}^{-1}$  corresponding to the asymmetrical and symmetrical stretching vibration of propyl groups, the peak at  $1201\text{ cm}^{-1}$  ascribed to the ether  $\text{C-O-C}$  stretching, and the peak at  $910\text{ cm}^{-1}$  assigned to stretching vibration of epoxy ring, which is in consistent with GPTMS spectrum<sup>8-10</sup>. More importantly, the enhanced absorption band at  $1100\text{ cm}^{-1}$  for  $\text{GT}_{50}$  and  $\text{GS}_{50}$  nanocomposites, which represents the asymmetrical stretching vibration of linear  $\text{Si-O-Si}$ , indicated that the hydrolyzed GPTMS has undergone condensation among themselves to achieve an organosilicate network<sup>11</sup>. The FTIR



results are in consistent with the XPS analysis. Thus, it is conducive to improve the robustness of the hybrid film against cracking formation.

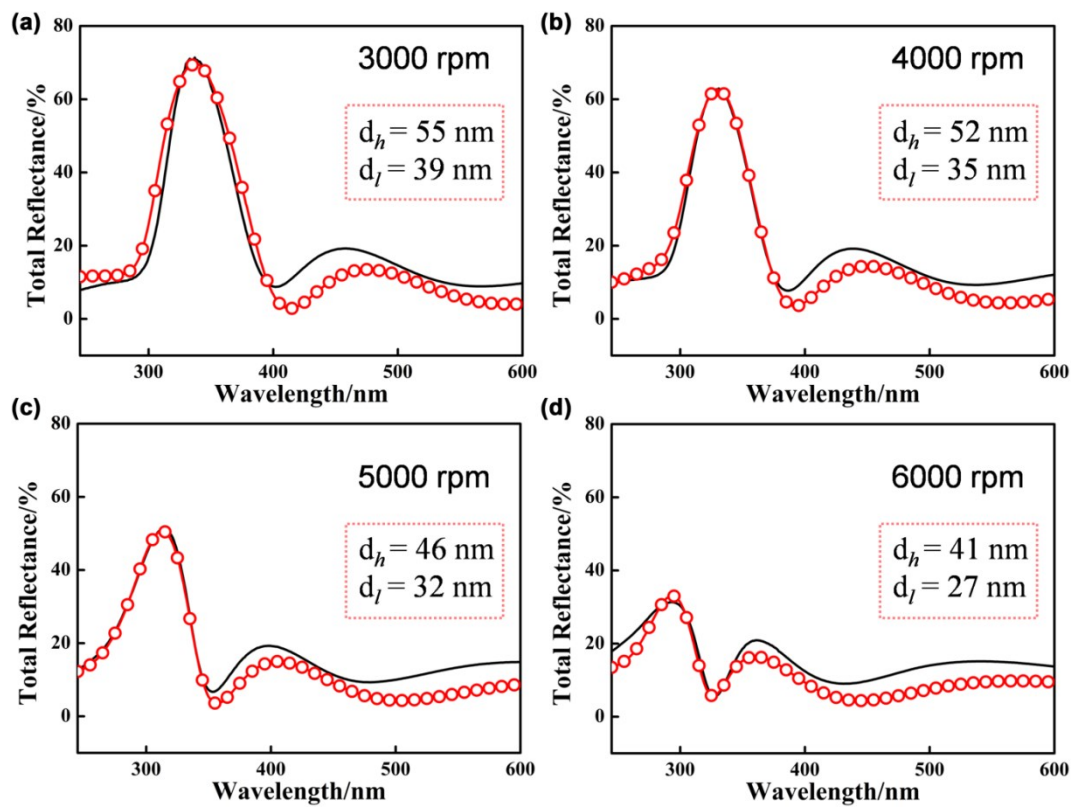


**Fig. S6** Measurement and simulation of reflectance spectra of GTS<sub>50</sub> 1DPhC films coated PC prepared at different rotation speed ranging from 3000 rpm to 6000 rpm. The fitted thicknesses for their corresponding high refractive index layer and low refractive index layer were given in the inset red rectangle respectively.

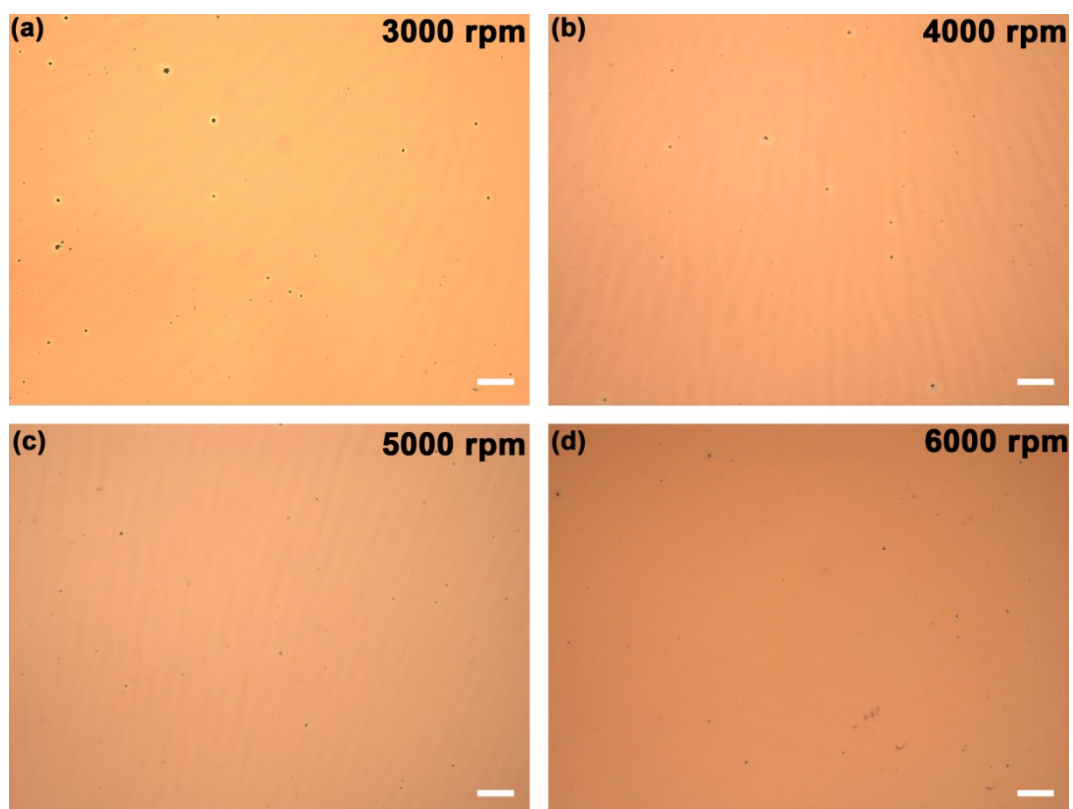


**Fig. S7** Optical images of GTS<sub>50</sub> 1DPhC films coated PC prepared at different rotation speed of (a) 3000 rpm, (b) 4000 rpm, (c) 5000 rpm and (d) 6000 rpm (scale bar = 100  $\mu\text{m}$ ).

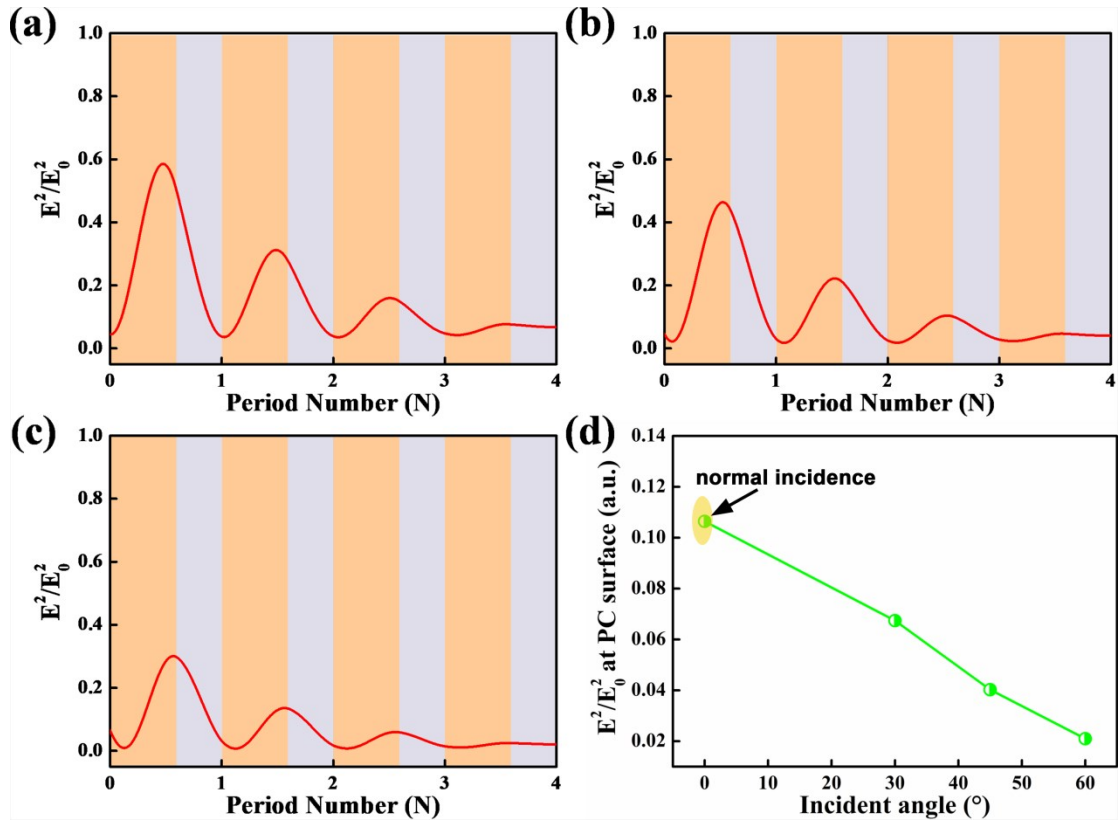


**Fig. S8** Spatial distribution of electric field,  $E^2/E_0^2$ , along the cross section of the GTS<sub>50</sub> 1DPhC film prepared at 5000 rpm, for the light of wavelength at 313 nm with different incident angles: (a) 30°, (b) 45° and (c) 60°, (d) the  $E^2/E_0^2$  values at PC surface under different light incident angles.

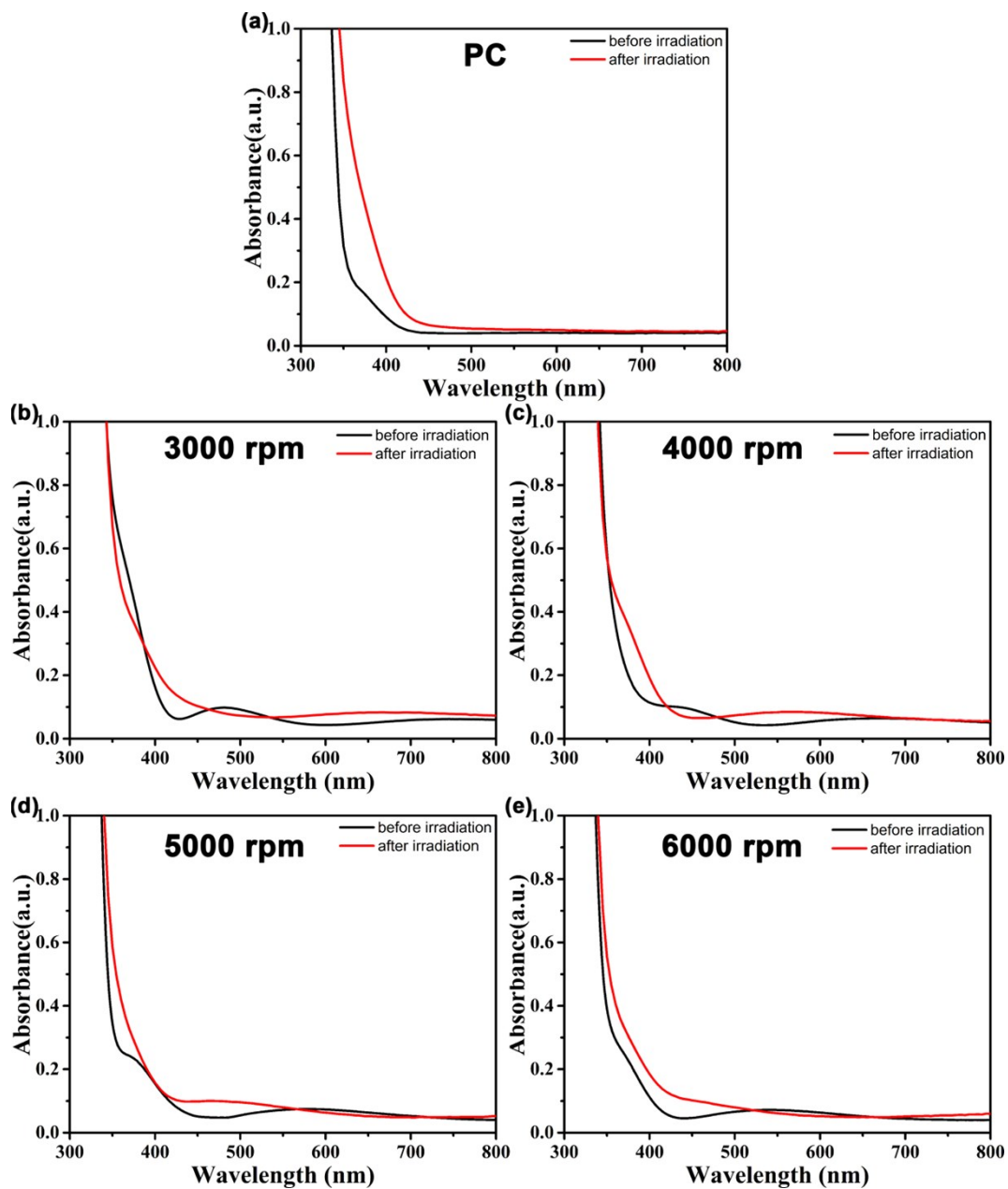


**Fig. S9** Absorbance spectra of bare PC (a) and GTS<sub>50</sub> 1DPhC films coated PC prepared at different rotation speed of (b) 3000 rpm, (c) 4000 rpm, (d) 5000 rpm and (e) 6000 rpm, which were measured both before and after UVB irradiation.

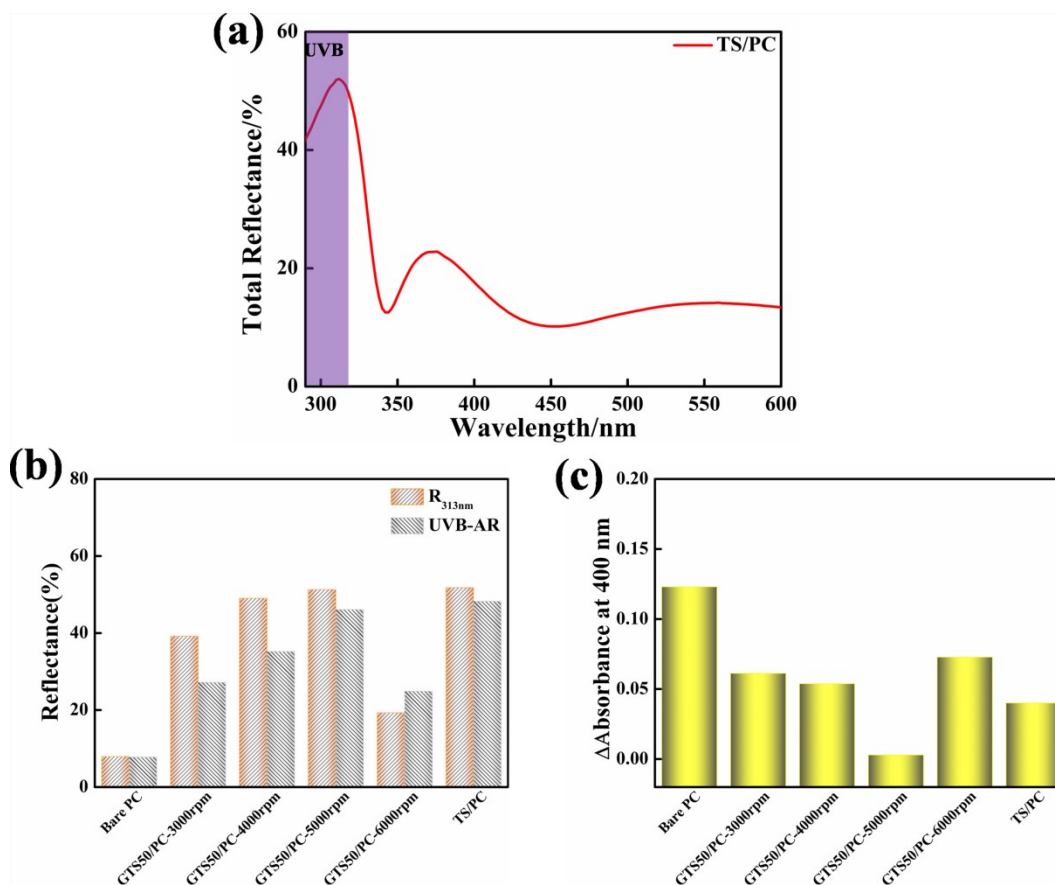


**Fig. S10** (a) Total reflectance spectrum for the TS/PC sample; (b) the reflectance at wavelength of 313 nm ( $R_{313nm}$ ) and UVB-AR of bare PC, TS/PC and GTS<sub>50</sub>/PC samples; (c) the absorbance change at 400 nm after UVB aging for bare PC, TS/PC and GTS<sub>50</sub>/PC samples.

For comparison, the optical property and photoprotection performance of conventional TS/PC was also analyzed. It was clear that the reflectance at wavelength of 313 nm and the average reflectance in the UVB region of the TS/PC sample were nearly the same as that of the GTS<sub>50</sub>/PC sample prepared at 5000 rpm. As expected, the absorbance change at 400 nm, which indicated the degradation of PC substrate, of TS/PC as well as GTS<sub>50</sub>/PC prepared at 5000 rpm were lower than that of other samples. Nonetheless, the absorbance change at 400 nm of GTS<sub>50</sub>/PC sample prepared was much lower than that of TS/PC sample after UV aging test, suggesting that the GTS<sub>50</sub> 1DPhC film had superior photoprotection effect. This may be because

the surface cracks on TS 1DPhC film expedited the contact of oxygen and UV light with the substrate, which led to a more serious photo-oxide degradation of PC than the crack-less GTS<sub>50</sub> 1DPhC film coated PC.

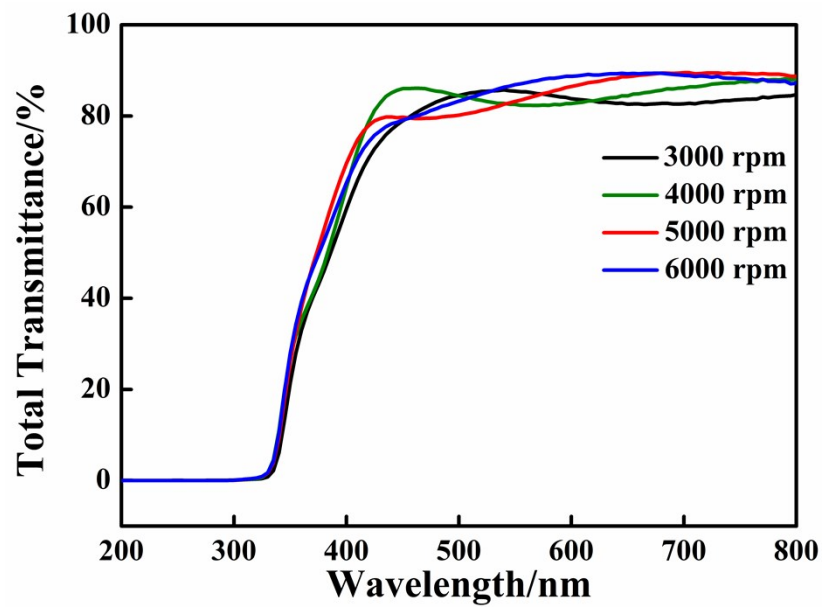


**Fig. S11** The transmittance spectra of GTS<sub>50</sub>/PC samples after UVB irradiation test



## References

1. David P. Landau and K. Binder, *A Guide to Monte Carlo Simulations in Statistical Physics*, Cambridge University Press, Cambridge, UK, 2005.
2. G. M. Paterno, C. Iseppon, A. D'Altri, C. Fasanotti, G. Merati, M. Randi, A. Desii, E. A. A. Pogna, D. Viola, G. Cerullo, F. Scotognella and I. Kriegel, *Sci Rep*, 2018, **8**, 3517.
3. S. Xun, W. Zhu, Y. Chang, H. Li, M. Zhang, W. Jiang, D. Zheng, Y. Qin and H. Li, *Chem. Eng. J.*, 2016, **288**, 608-617.
4. L. Kasten, V. Balbyshev and M. Donley, *Prog. Org. Coat.*, 2003, **47**, 214-224.
5. A. Saleem, N. Ullah, K. Khursheed, T. Iqbal, S. Shah, M. Asjad, N. Sarwar, M. Saleem and M. Arshad, *J. Electron. Mater.*, 2018, **47**, 3749-3756.
6. J. Liu, Q. Yu, M. Yu, S. Li, K. Zhao, B. Xue and H. Zu, *J. Alloys Compd.*, 2018, **744**, 728-739.
7. U. Tiringier, I. Milosev, A. Duran and Y. Castro, *J. Sol-Gel Sci. Technol.*, 2018, **85**, 546-557.
8. S. Eshkalak, E. Kowsari, A. Chinnappan and S. Ramakrishna, *J. Mater. Sci.-Mater. Electron.*, 2019, **30**, 11307-11316.
9. Y. Zhang, S. Shen, S. Wang, J. Huang, P. Su, Q. Wang and B. Zhao, *Chem. Eng. J.*, 2014, **239**, 250-256.
10. S. Matavos-Aramyan, *Silicon*, 2018, **10**, 1601-1612.
11. F. Peng, L. Lu, H. Sun, Y. Wang, J. Liu and Z. Jiang, *Chem. Mater.*, 2005, **17**, 6790-6796.